Making seismic monitoring work in a complex desert environment — 4D processing

Robert Smith[1], Emad Hemyari[1], Andrey Bakulin[1], and Abdullah Alramadhan[1]

https://doi.org/10.1190/tle38080637.1.

Abstract

Seismic monitoring of an onshore carbonate reservoir in a desert environment has been achieved for the first time. Optimizing data repeatability was key to detecting the weak 4D (time-lapse) signal resulting from a fluid-injection program, which was achieved through a combination of specialized survey design, careful acquisition, and dedicated 4D processing. The hybrid acquisition system utilized buried geophones, which significantly reduced 4D noise caused by variability in the near-surface environment. Despite the extensive acquisition efforts, time-lapse processing is an essential component of achieving highly repeatable data. A fit-for-purpose workflow was developed to reduce the remaining 4D noise using a combination of parallel and simultaneous processing. Processing steps leading to the largest improvement in reflection signal-to-noise ratio, such as noise attenuation, amplitude balancing, and supergrouping, produced the largest reduction in 4D noise. Outstanding final migrated data repeatability has been achieved, comparable to levels reported for the more favorable permanent marine systems. However, the need to use surface sources results in a seasonal imprint on data repeatability, which hinders the interpretation of surveys acquired during different seasons. In the absence of a fully buried acquisition system, advanced processing techniques such as surface-consistent matching filters may be required to resolve these variations.

Introduction

Reservoir management can be enhanced through the integration of time-lapse seismic data, which can improve our understanding of dynamic reservoir processes and the volumetric distribution of injected fluids. Although seismic monitoring has been implemented by numerous projects, the majority of successes have been for offshore clastic reservoirs where time-lapse seismic conditions are most favorable. The number of onshore monitoring ventures are steadily increasing (e.g., Ketzin [Ivanova et al., 2012], Aquistore [Roach et al., 2015], and Otway [Pevzner et al., 2017]) but predominantly focus on clastic reservoirs, which produce relatively large 4D signal in comparison to carbonates. The Weyburn Field in Canada (Meadows and Cole, 2013) is the only known dedicated monitoring of an onshore carbonate reservoir reported so far. However, the complex and time-variant nature of near-surface geology in arid environments, such as that encountered in this study, can potentially generate much higher levels of 4D noise. A hybrid acquisition scheme consisting of buried receivers and surface vibroseis sources was implemented to reduce the effect of the near surface. Despite this, 4D processing is another essential component for minimizing 4D noise, particularly given the point-source point-receiver nature of the acquisition. This article focuses on the development of the 4D processing workflow that has resulted in highly repeatable data for monitoring of an onshore carbonate reservoir.

Achieving seismic monitoring of onshore carbonate reservoirs in a desert environment

Until now, seismic monitoring of onshore carbonate reservoirs in desert environments has remained one of the last time-lapse seismic frontiers. The stiff rock frame typical of carbonates results in low sensitivity to changes in reservoir conditions and subsequently small variations in seismic reflections (4D signal). The search for weak 4D signal is compounded in arid locations by the complex near-surface geology, where thick sand dunes and karsts hinder even conventional imaging due to the generation of strong ground roll and backscattered noise, respectively. For time-lapse surveys, we face the additional challenge of near-surface variations over time, which are a major source of 4D noise. For instance, sand dune migration results in vertical shifts of up to half a meter per year, while seasonal weather trends also increase 4D noise significantly (Bakulin et al., 2018b). To enable detection of the small time-lapse signal expected (acoustic impedance change of 3%–6%), sources of 4D noise should be minimized as far as possible through a combination of specialized survey design, careful acquisition, and fit-for-purpose processing.

Design and acquisition. A fully buried acquisition system would avoid many of the issues posed by the shallow near surface but is currently inadequate for imaging the reservoir of interest (Berron et al., 2012). The final survey design employed a hybrid system using buried sensors and surface sources (Figure 1), which was found to be the best compromise for imaging and data repeatability. Key to this system was the use of 1003 buried (50–80 m) three-component (3C) geophones, which reduce time-lapse noise introduced by variable near-surface conditions (Bakulin et al., 2012). At the surface, a dense (10 × 10 m) grid of vibroseis shot points (Figure 1b) was used to ensure unaliased sampling of coherent noise. A single vibrator was used per shot point, effectively generating point-source point-receiver data. Source points were repositioned with a high degree of accuracy using a differential GPS guidance system, resulting in mean positioning errors of just 0.3 m (Bakulin et al., 2016). Dense source sampling produced high-fold data (maximum of 900, Figure 1c), which enhance reflection signal-to-noise ratio (S/N), a factor which can also improve repeatability (Pevzner et al., 2011). Continuous data acquisition produced one full survey every four weeks, with data from 37 surveys recorded over a 34-month period included in this article.

[1]Saudi Aramco, EXPEC Advanced Research Center, Dhahran, Saudi Arabia. E-mail: robsmith155@gmail.com; emad.hemyari@gmail.com; andrey.bakulin@aramco.com; abdallah.ramadan@aramco.com.

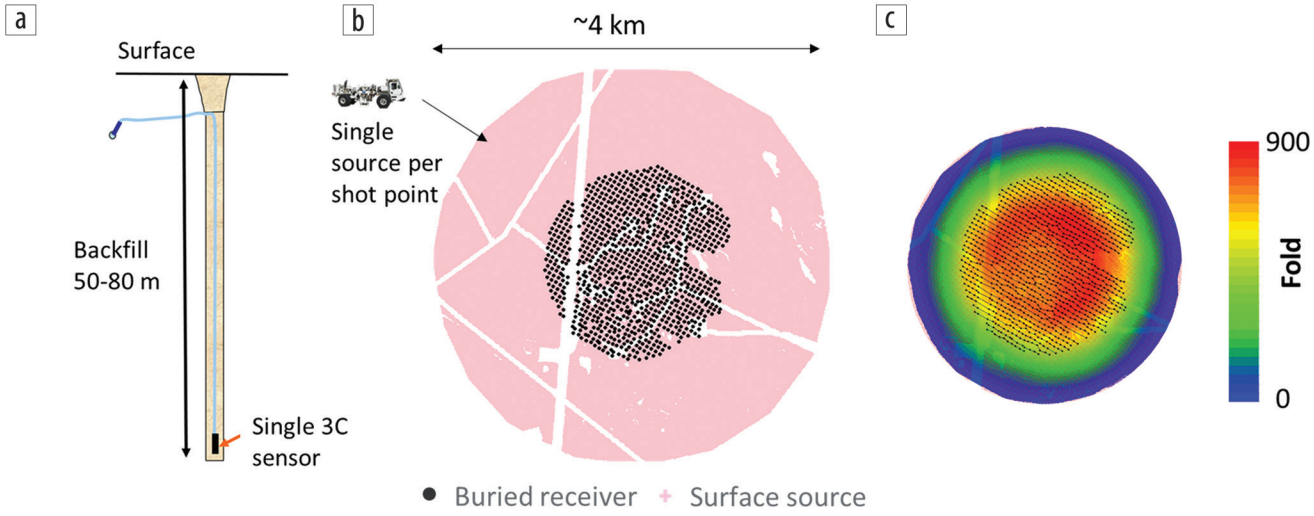

Figure 1. Final survey design showing (a) geophones buried 50–80 m beneath the surface, (b) overview of the single-source single-receiver layout, and (c) resulting high-fold data distribution (5 × 5 m bins).

Time-lapse seismic processing challenges. In addition to the considerable acquisition efforts, data processing was required to account for the unique survey design and remaining 4D noise. Figure 2 summarizes some of these challenges. Although receivers are placed 50–80 m below the surface, the reflections of interest (blue arrows, Figure 2a) are masked by strong coherent noise resulting from mode conversions, guided waves, and refracted arrivals. The installation depth means that ground roll, which is likely more susceptible to near-surface variations, is largely attenuated. Therefore, the noise characteristics do not appear to vary noticeably between seasons. Noise attenuation is essential to uncover the reflection events. Additionally, the point-source point-receiver nature of the acquisition (Figure 1), and inherent low reflection S/N, has important implications for the processing methodology.

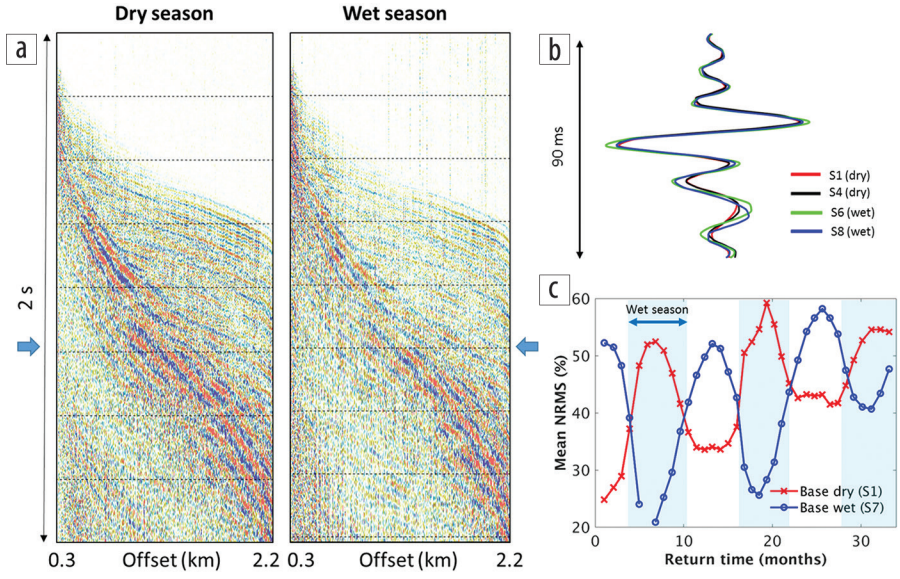

Figure 2. Processing challenges for time-lapse data acquired in desert environments. (a) High-amplitude coherent noise obscures reflection events of interest (blue arrows), while (b) seasonal variations contaminate the data as demonstrated by the early arrivals recorded by a single source-geophone pair. (c) The average early-arrival NRMS return curves for two baselines acquired in different seasons exhibit the cyclical nature of data repeatability.

The need for surface sources means the data are still sensitive to the constantly evolving near-surface environment (Bakulin et al., 2018b). This is apparent in Figure 2b where early-arrival waveform changes corresponding to seasonal climatic variations are observed. The two dry-season traces (red and black), produced from the same source-receiver pair during different surveys, match almost perfectly. The equivalent traces from two surveys acquired during the cooler, wetter part of the year (blue and green traces) show subtle but significant deviations. Although the differences appear to be small, they are of similar magnitude to the 4D signal we are trying to measure.

The level of 4D noise can be quantified using the normalized root-mean-square (NRMS) attribute proposed by Kragh and Christie (2002) in which increasing values indicate degrading repeatability. The nearest offset trace from each shot record is selected, and the NRMS is computed on a 50 ms window below the first-break pick. The resulting mean early-arrival NRMS is plotted in Figure 2c using two baseline surveys. Survey one (red line) was acquired during the dry summer months, while survey seven (blue line) is from the first wet season. Clear cyclical variations in the data repeatability are apparent, with 4D noise minimized when comparing surveys acquired under similar climatic conditions (i.e., dry-dry or wet-wet).

4D seismic processing of onshore buried receiver data

Despite increasing numbers of onshore time-lapse seismic projects, only a few publications on land 4D processing exist in the literature (e.g., Li et al., 2012; Meadows and Cole, 2013; Bergmann et al., 2014; Roach et al., 2015). Although the challenges

and overall workflow applied to land and marine time-lapse surveys may differ somewhat, the guiding principles remain the same. In general, processing algorithms and parameters should be kept identical for all surveys (Johnston, 2013). For instance, a common stacking velocity is used because the process of repicking may introduce larger errors than what we are trying to correct for.

Three approaches exist for processing time-lapse data: (1) process each survey independently using unique flow/parameters; (2) process each vintage in parallel using the same flow and parameters; or (3) the simultaneous method defined by Lumley et al. (2003) in which multivintage data sets are combined and processed as one (referred to as joint processing by Meadows and Cole [2013]). An overview of the workflow applied in this study is shown in Figure 3a, which used a combination of parallel and simultaneous processing. Whereas the aim of conventional processing is to generate the best image, here we have the additional objective of optimizing repeatability between surveys. These two goals often work together, but when they do not, repeatability is prioritized. Care must be taken to ensure the desired 4D signal is not harmed in the process of trying to match surveys.

To guide the workflow and parameter selection, the background NRMS was computed on stacked data after each processing step. Generally, a process or parameter selection is only acceptable when mean repeatability is improved. The average NRMS progression for the final processing workflow (computed in the reservoir window but excluding zones where 4D signal was expected) is given in Figure 3b for two survey combinations. Surveys one and two were acquired a month apart in similar (dry and hot) climatic conditions, while survey seven was from a much cooler and wetter time of year. This highlights the increased 4D noise when comparing surveys from different seasons, although 4D processing reduces the gap considerably when compared to data with only preprocessing applied.

Data preparation. A number of preprocessing steps were applied to improve data quality and maximize the similarity between baseline and monitor surveys. First, survey geometry was equalized by dropping shots and receivers that were not present in all data sets. For each of the 37 vintages covered in this article, 101,518 shots and 913 receivers were included in the final results. Although additional rejection of nonrepeatable shot records (identified using early-arrival repeatability analysis) resulted in significant improvements for the 2D feasibility tests (Bakulin et al., 2015), it had little impact for the full 3D monitoring data sets. Since the same early-arrival analysis was used as an in-field quality-control tool, any major acquisition issues were quickly identified and resolved (Bakulin et al., 2016). In addition, each shot only contributes to 913 traces, so highly nonrepeatable shots are generally less of an issue. Conversely, receivers that change response over time must be removed since one geophone contributes to a larger proportion of the data and has a major impact on the final output. Other preprocessing steps included sensor rotation to correct for nonvertical placement of the downhole 3C geophones, spherical divergence correction, and removal of monofrequency noise (50 and 60 Hz). Each of these steps was applied using the same algorithms and parameters for each survey.

Full datum statics were also applied early in the workflow to avoid processing with shots and receivers at significantly different elevations. While this is not the conventional approach, the impact should be minimal due to the lack of far-offset data. Although arrival-time differences are introduced by changes in near-surface velocity and topography over time, the same datum static corrections are applied to all surveys. Similar to Bergmann et al. (2014), we attempt to account for these time shifts between surveys later in the processing workflow using a modified version of surface-consistent residual statics. An alternative option implemented by

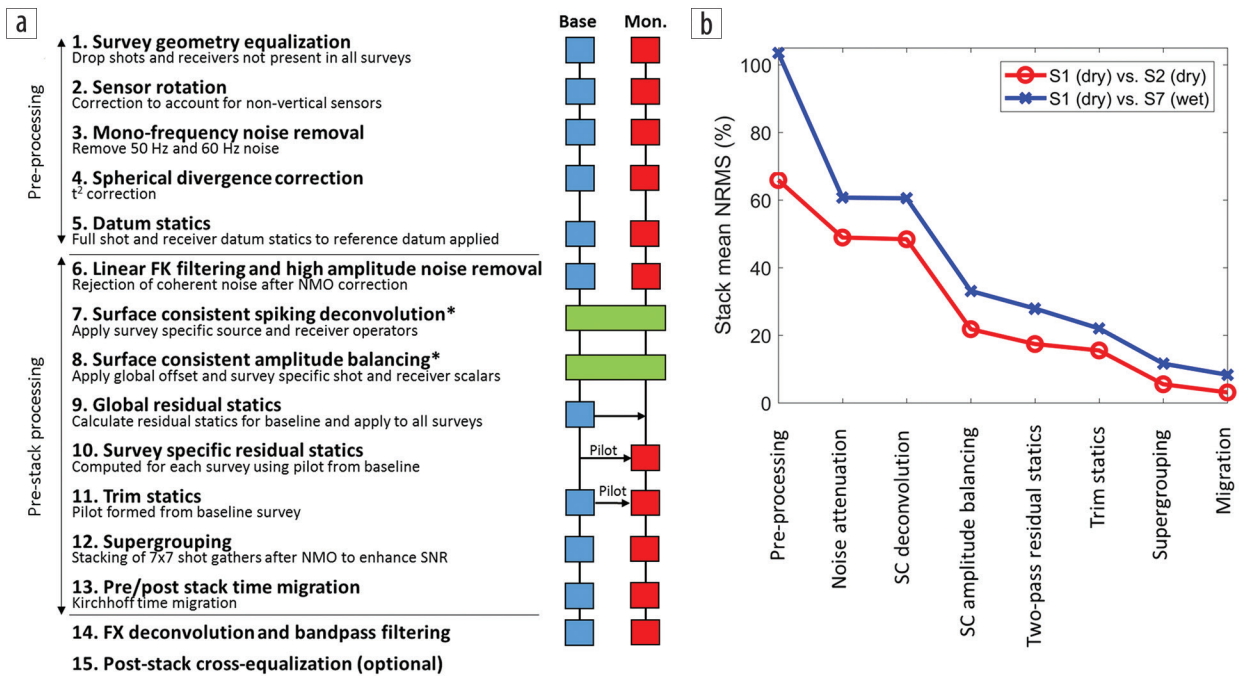

Figure 3. (a) General workflow using a combination of parallel and simultaneous (denoted with *) processing. (b) Mean stack NRMS progression curve measured in the reservoir window for two survey combinations.

Pevzner et al. (2011) is to rederive the near-surface model for each survey using refraction tomography. This is not a viable option with monthly data sets however, and refraction tomography is unlikely to provide the accuracy required for these small corrections.

Noise attenuation. As highlighted in Figure 2a, the raw data are contaminated by strong coherent noise with apparent velocity that does not vary noticeably between seasons. Therefore, localized F-Kx-Ky filtering was applied after normal moveout correction in the densely sampled common-receiver domain to each survey in parallel (i.e., using the same rejection parameters). A median filter in the time-frequency domain was also employed to remove high-amplitude noise bursts.

Figure 4 shows the impact of the processing workflow on an example common-depth-point (CDP) gather. Comparing the gathers before and after noise attenuation in Figures 4a and 4b, respectively, the reflection events become more evident after denoising but are still weak due to the single-source single-receiver nature of the acquisition. The bottom row of Figure 4 shows the repeatability progression of the example gather using a sliding window (100 ms) NRMS calculation between the first two surveys. Here the repeatability appears to degrade after the application of noise removal (Figure 4f), but this results from measuring weak reflection events after the removal of strong and repeatable coherent noise. The mean stack NRMS shown in Figure 3b shows the true impact of noise attenuation, with a large improvement in stack repeatability for both survey combinations compared to only applying basic preprocessing.

Surface-consistent deconvolution and amplitude balancing. Spatial and temporal variations in source and receiver coupling can contribute significantly to 4D noise, as demonstrated by the seasonal repeatability trends shown in Figure 2c. We attribute most of this nonrepeatability to the source side since the receivers are buried deep beneath the surface. To address these changes, a simultaneous surface-consistent deconvolution and amplitude-balancing approach was implemented in which all surveys are merged and processed as one data set. As discussed by Li et al. (2012), this multivintage technique can be better thought of as source and receiver consistent processing. Rather than applying a constant deconvolution operator or scaling factor for a specific surface location, unique keys are assigned to each shot/receiver for every survey to allow operators/scalars to vary over time. The four-term decomposition is completed by global offset and CDP terms.

Spiking deconvolution was applied using the derived source and receiver operators to correct for wavelet distortions. Bandwidth

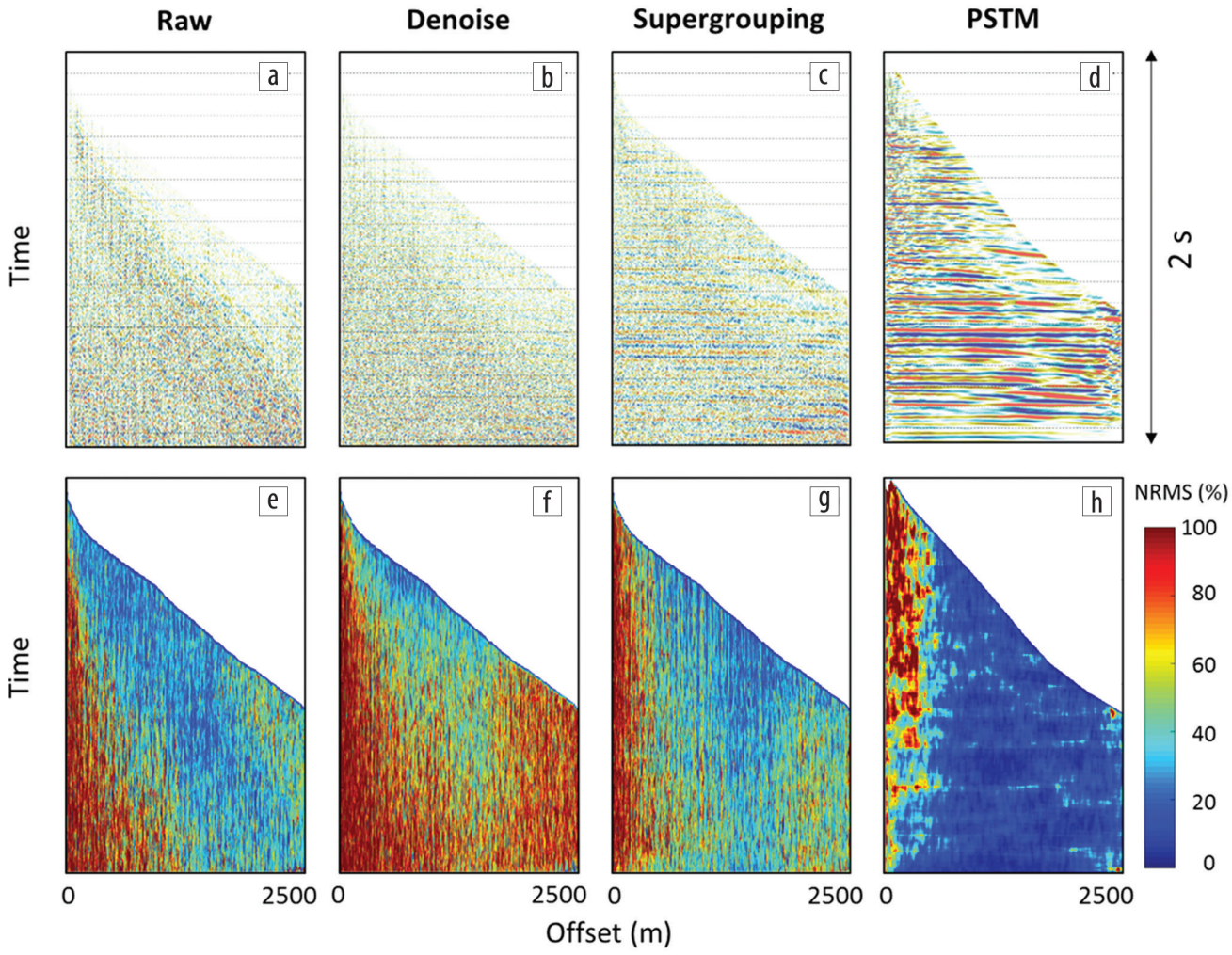

Figure 4. Example CDP gather (top) and repeatability (bottom) at different stages of the processing workflow: (a,e) raw gather, (b,f) after linear and high-amplitude noise attenuation, (c,g) after supergrouping, and (d,h) final migrated gather. Note gathers are shown with trace scaling applied.

was restricted (10–60 Hz) to avoid boosting higher frequencies that are known to be less repeatable. The multisurvey version of classical surface-consistent amplitude-balancing attempts to recover and correct for source and receiver scaling factors both within an individual survey and between different vintages (Bakulin et al., 2018c). Since the expected 4D signal is predominantly an amplitude feature, the analysis was restricted to a 600 ms window above the reservoir. The measured amplitudes were then decomposed to source and receiver consistency using a Gauss-Seidel iterative procedure. Examples of the survey-specific source scalars are shown in Figures 5a and 5b for surveys one and seven, respectively. The near-surface geology is reflected in each scalar map, but subtle differences (Figure 5c) may reflect variations in coupling and near-surface conditions. The global offset (Figure 5d) and survey-specific source and receiver scalars were then applied to the data. Figure 5e shows the mean rms amplitude for each survey measured in the overburden window, which shows that cyclical variations in the data were removed after the application of amplitude scalars.

The impact of this multisurvey processing on stacked data repeatability is shown in Figure 3b. Amplitude balancing results in a large reduction in 4D noise, more than halving the NRMS for both survey combinations. The global offset scaling term (Figure 5d) accounts for a sizable proportion of this improvement since the data prior to balancing are largely dominated by noisy and high-amplitude near-offset traces that control the stacked output. By suppressing near-offset traces and scaling up mid to far offsets, we effectively boost the reflection S/N. Although Figure 3b appears to show that deconvolution had negligible impact on repeatability, this is misleading. Tests with deconvolution omitted from the workflow resulted in final NRMS (i.e., after migration) values that were approximately double what is reported in this article. This is likely due to improved performance of later processing steps as a result of better-quality input data when deconvolution is included.

Residual statics. Sand dune migration and changes in near-surface properties lead to small time shifts between different vintages of seismic data. Here we accounted for these variations using a two-pass surface-consistent residual statics workflow. The first pass was computed using the baseline survey to correct for near-surface complexity not captured in the datum statics model. These calculated shot and receiver statics were then applied to each survey as a global correction. The second pass was a survey-specific correction designed to remove the time-lapse shifts between baseline and monitor surveys. The survey-specific statics were calculated by crosscorrelating prestack traces from each monitor survey with stacked pilot traces from the baseline survey. These shifts were then decomposed in a surface-consistent manner, with the source and receiver terms applied to align each monitor

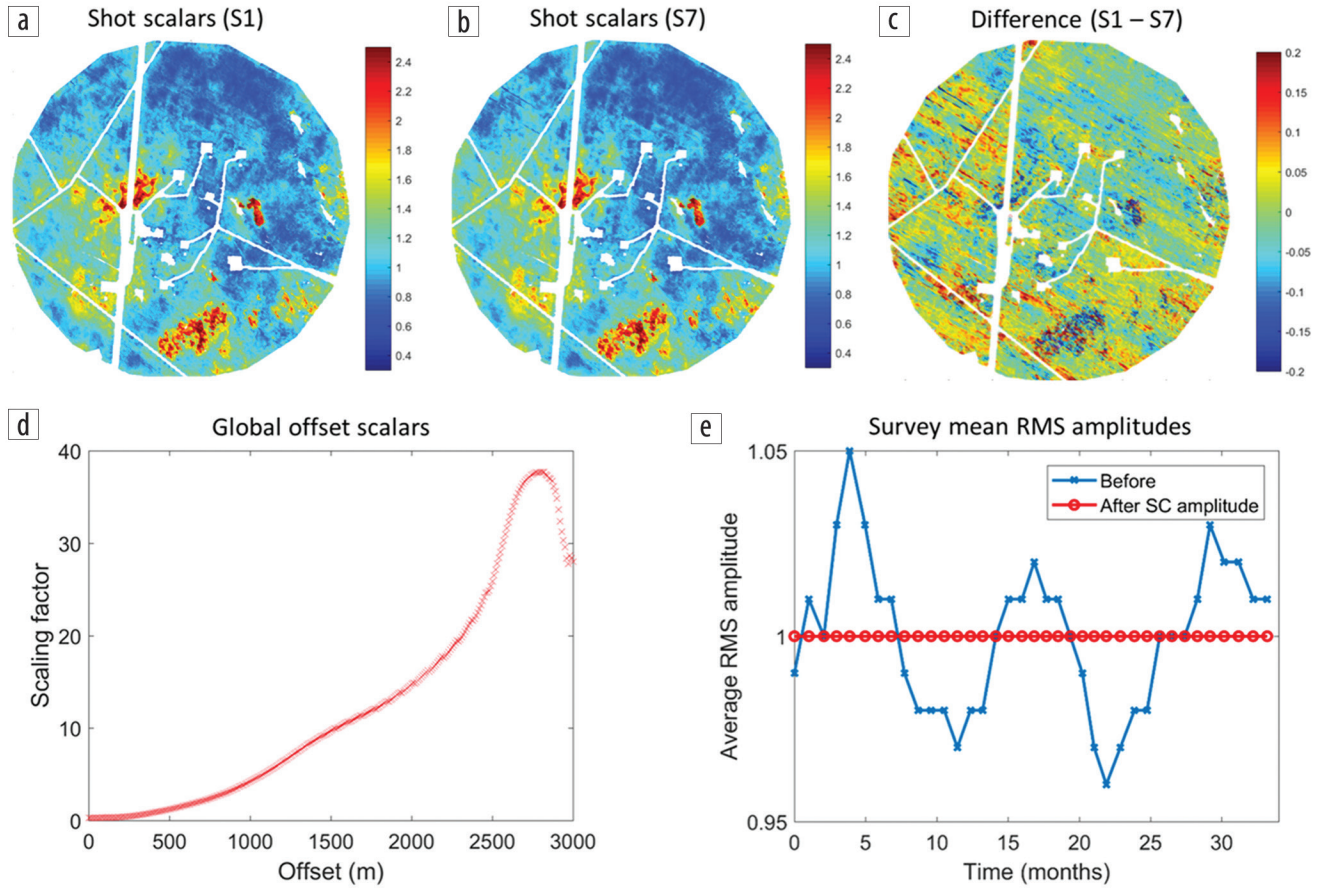

Figure 5. Examples of the survey-specific shot scalars derived using multivintage surface-consistent amplitude decomposition for (a) survey one, (b) survey seven, and (c) the difference between them. (d) A global offset scalar term is derived from the decomposition and applied to all surveys. (e) Mean rms amplitudes measured in an overburden window before and after the application of surface-consistent amplitude balancing.

survey with the baseline. This is a modified version of the approach implemented by Bergmann et al. (2014), who crosscorrelate prestack traces from the baseline and monitor surveys. This may not be the best approach in our case, owing to the lower S/N of the data.

Trim statics. As highlighted by Johnston (2013), caution should be exercised when applying trim statics to time-lapse data to ensure the signal of interest is not removed. In this case, the expected 4D signal is largely an amplitude effect, with maximum time shifts of 0.6 ms predicted based on modeling. To derive the trim static corrections, a pilot trace for each CDP was first constructed from the baseline survey. These pilot traces were used to compute and apply trim static corrections (maximum correction of two samples) in parallel for each monitor survey.

The application of trim statics was carefully analyzed for this study, paying particular attention to the reservoir zone and the effect on areas where 4D signal is expected. Time-lapse attribute maps were compared after processing the data through the entire workflow (i.e., after migration) with and without trim statics applied. It was concluded that anomalies in regions where 4D signal was expected were maintained when trim statics were included, while spurious effects away from the region of interest were suppressed. The improvement in stack repeatability (Figure 3b) is likely due to enhanced coherency of reflection signal within each survey and better alignment between surveys.

Supergrouping. The acquisition design, in which each trace is the result of a single source and receiver pair, results in low reflection S/N (Figure 4b). To enhance reflections and suppress remaining coherent and random noise, a method of digital array forming known as supergrouping (Bakulin et al., 2018a) was applied. In this method, neighboring shot gathers surrounding a central shot location are stacked to form a supershot gather (Figure 6a). Summation is applied after application of normal moveout correction, which helps preserve reflections and filter out the remaining noise. This process can be thought of as applying a sliding spatial averaging window to the data, with the enhanced gather output at the central shot location. Note that the output geometry is identical to the input data.

Different array sizes were tested to determine the effect on data quality and poststack repeatability (Figure 6b). A large

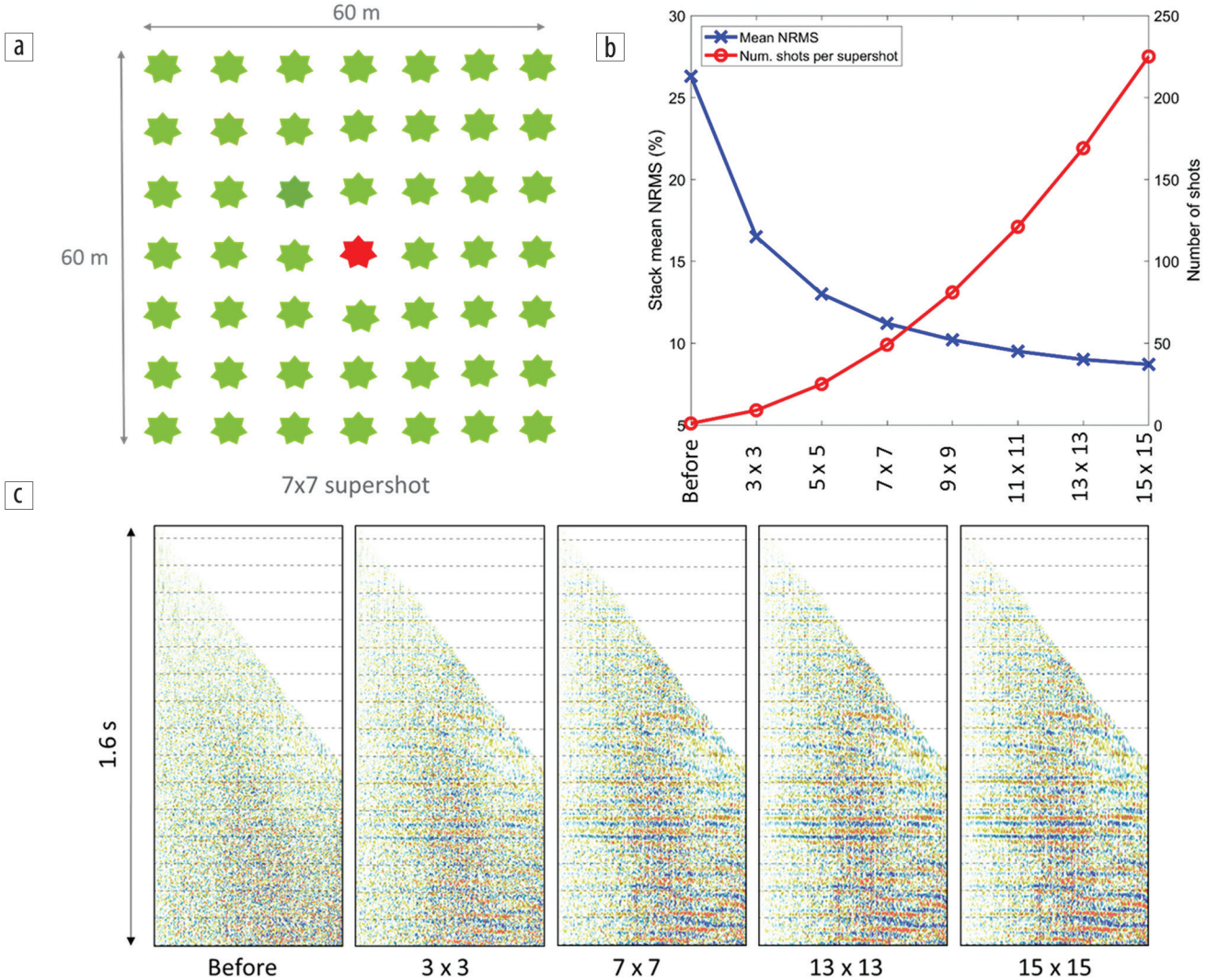

Figure 6. Effect of supergrouping on data quality and repeatability. (a) Example 7 × 7 supershot (red) geometry produced by stacking neighboring shots (green). (b) Impact of supergrouping array size on mean stack NRMS, and (c) data quality for an example CDP gather (gathers shown using a global scale).

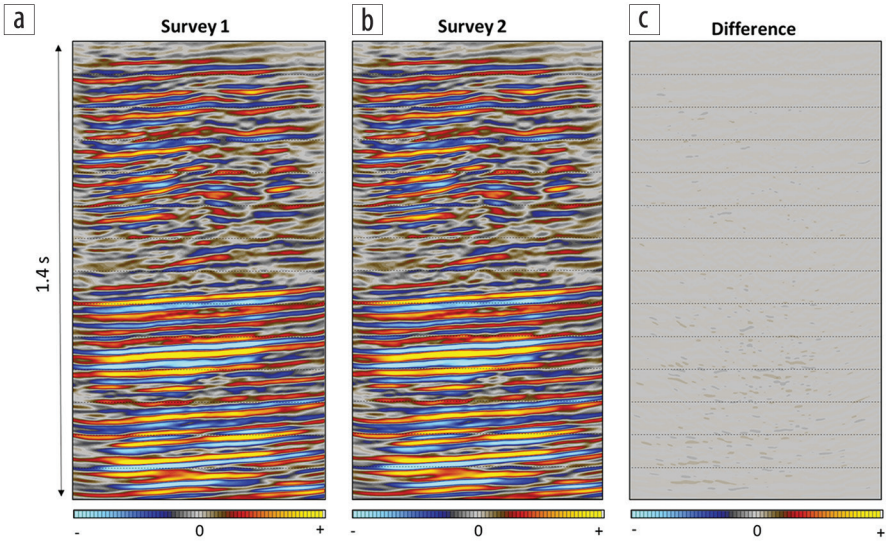

Figure 7. Example section from the final migrated volume for (a) survey one, (b) survey two, and (c) the difference between them. Plots are shown using a global scale.

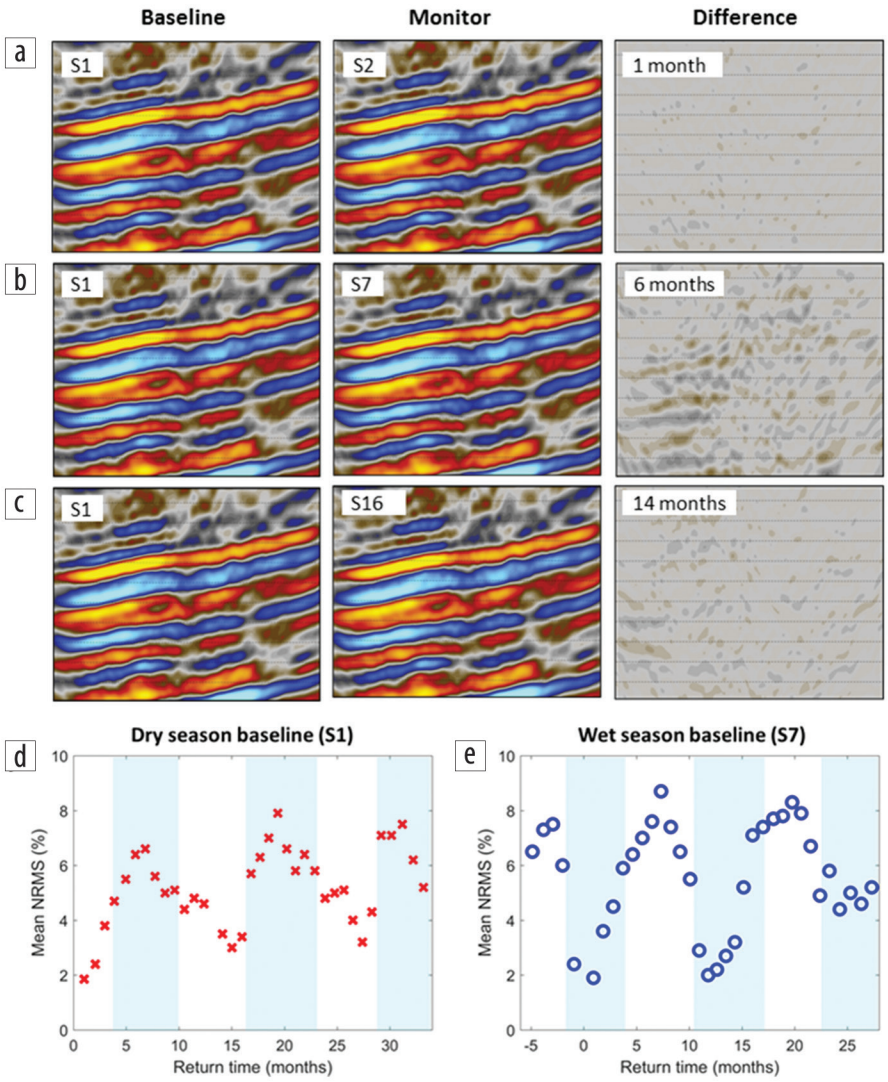

Figure 8. A zoomed section at the reservoir level showing 4D noise between (a) survey one and survey two (dry-dry), (b) survey one and survey seven (dry-wet), and (c) survey one and survey 16 (dry-dry). Seasonal repeatability trends shown by the mean stack NRMS computed at the reservoir level using (d) a dry- and (e) wet-season baseline survey.

reduction in mean NRMS is found using even a small 3 × 3 shot array (stacking of nine shot gathers), reducing the average from 27% to 16%. Further improvements are observed with increasing group size, although the reduction becomes less significant with larger shot groups and starts to plateau with an array size of 11 × 11 shots. The effect of different array sizes on data quality is shown for an example CDP gather in Figure 6c. Reflections are difficult to distinguish prior to supergrouping but are significantly enhanced through the process of stacking neighboring shots.

For the final workflow, an array size of 7 × 7 shots was selected as the best choice for enhancing repeatability while limiting the effects of lateral smearing. The effect of supergrouping on the repeatability of the example CDP gather (Figure 4g) shows substantial improvements compared to data that are not supergrouped.

Migration. Either prestack or poststack Kirchhoff time migration can be applied for the final data using a common velocity model for all surveys. While prestack migration (PreSTM) may yield slightly better repeatability results, the computation time required is substantially greater. PreSTM results in considerable improvement to the example gather shown in Figure 4d as well as reducing the NRMS in most areas of Figure 4h. Even after the full processing flow, the near-offset traces remain highly nonrepeatable. This may be caused by reverberations in the near surface resulting from energy trapped within sand dunes and between layers with high impedance contrasts. Therefore, near-offset traces are muted for the final stack output.

Poststack processing. A bandpass filter was applied to the data after stacking, followed by an F-XY deconvolution to reduce random noise in the final output. Note that the results in this article do not include application of poststack cross-equalization. With very high levels of repeatability already achieved, further cross-equalization did not produce any major improvements in data similarity so is not currently included. The remaining seasonal

imprint on data repeatability is important (see next section) but may need to be corrected prestack.

Final image and repeatability

A section from the final image volume is shown in Figure 7 for the first two surveys. The difference section (Figure 7c) demonstrates the highly repeatable nature of the data. Figures 8a–8c show a zoomed section around the reservoir of interest (but away from regions expected to be affected by 4D signal) for different baseline and monitor survey combinations to show how the 4D noise varies over time. Comparing the first two surveys (Figure 8a), which are both acquired in the summer and separated by only one month, the 4D noise is very low and barely noticeable on the difference section. A considerable increase in 4D noise is observed after six months (Figure 8b) when the monitor survey was acquired during the wet, cooler period of the year. When conditions return to hot and dry the following year, the two sections once again have high similarity (Figure 8c).

Seasonal trends in data repeatability are represented by the mean stack NRMS return curves shown in Figures 8d and 8e for a dry and wet season baseline, respectively. This is calculated within the high-fold (> 300) areas of the reservoir window but excluding regions where 4D signal is expected. Results shown are after applying a 12–30 Hz bandpass filter, which was found to provide the optimum repeatability (12–60 Hz data generally result in NRMS values 1%–2% higher). Outstanding repeatability is observed when comparing surveys acquired under similar climatic conditions, with mean NRMS values of 2%–3% achieved even after several years. This level of repeatability, which is similar to background NRMS values reported for offshore permanent reservoir monitoring schemes (e.g., Ekofisk [Bertrand et al., 2014]), has enabled 4D signal related to fluid injection to be observed (Bakulin et al., 2018b). Some of the seasonal 4D noise that was observed in the early-arrival data (Figure 2c) remains. Due to the weak 4D signal, this means that surveys acquired in different seasons cannot be compared for the interpretation process. One solution to allow the full data set to be used is to adopt multiple baseline surveys (e.g., surveys one and seven) corresponding to the different seasons.

Discussion

The use of a novel acquisition system and dedicated 4D processing has resulted in highly repeatable seismic data. Although 4D processing reduces the time-lapse noise between surveys acquired in different seasons (Figure 3b), a seasonal imprint remains. This prevents the difference volumes from surveys acquired under different climatic conditions from being used for interpretation, since the increased 4D noise masks the small time-lapse signal. One approach that may improve future processing is the application of surface-consistent matching filters (Almutlaq and Margrave, 2013), which inherently attempt to correct for amplitude, phase, and time shifts between baseline and monitor surveys. In the current workflow, the surface-consistent deconvolution and amplitude-balancing steps have no objective to match the monitor surveys to the baseline. In the absence of improved processing methods, this suggests that surveys should be designed with multiple baseline surveys acquired during different seasons. Alternatively, future advances in buried source technology may enable this surface-related 4D noise to be avoided altogether.

The workflow outlined in this article uses a combination of parallel and simultaneous processing steps. While simultaneous processing may help reduce 4D noise, it can be a burden with frequent monitoring, as each new vintage requires reprocessing of all previous surveys. This can prevent timely delivery of results to engineers, with delays increasing as the number of data sets grows. One solution may be to have an additional version of processing in which all steps are run in parallel, which only requires processing of the new data set. The result is a much faster output for preliminary interpretation, which can also help identify any issues for the main (but slower) processing workflow.

Another important observation was made regarding the process of selecting the best method or parameters for each processing step. The choice leading to the largest immediate improvement in mean stack NRMS does not always result in the best final repeatability. For example, another powerful noise attenuation option using antileakage Fourier transform interpolation (Qin et al., 2018) was substituted for the localized FK filtering used in the current sequence. Although a much larger initial improvement in mean stack NRMS was evident, it failed to outperform our current workflow by the end of the processing sequence. We concluded that the alternative approach "manufactures" some amount of signal from the abundant noise. While these "signals" appear more robust, they do not consistently repeat between surveys, leading to reduced repeatability at the end. In contrast, supergrouping only stacks actual signals and does not generate similar artifacts. In the case of desert environments, which typically produce poor-quality data, processing steps that deal with data quality issues typically lead to the largest improvement in repeatability.

Summary

Seismic monitoring of onshore carbonate reservoirs in a desert environment is one of the last frontiers for time-lapse seismic. To overcome the high levels of 4D noise caused by varying near-surface conditions, a hybrid acquisition system using buried geophones has been deployed. While this significantly reduces 4D noise, specialized time-lapse processing is the second essential component that has resulted in highly repeatable data. Processing steps that enhance reflection signal, such as noise attenuation, amplitude balancing, and supergrouping, yielded the largest improvements in data repeatability. Seasonal variations of 4D noise between dry and wet seasons remains an issue and will need to be addressed with more advanced processing techniques or a fully buried acquisition system.

The combination of specialized acquisition design and fit-for-purpose 4D processing has resulted in excellent data repeatability with mean NRMS as low as 2%–3% recorded between surveys separated by more than one year. This level of repeatability has enabled monitoring of an onshore carbonate reservoir in a desert environment for the first time. TLE

Acknowledgments

We are grateful to many colleagues from Saudi Aramco who assisted with this project, in particular Mike Jervis, Kevin Erickson, Sergey Kishchik, Kurt Janssen, Ilya Silvestrov, Philippe Nivlet, and Mohammed Mubarak.

Data and materials availability

Data associated with this research are confidential and cannot be released.

Corresponding author: robsmith155@gmail.com

References

Almutlaq, M. H., and G. F. Margrave, 2013, Surface-consistent matching filters for time-lapse seismic processing: Geophysics, **78**, no. 5, M29–M41, https://doi.org/10.1190/geo2013-0049.1.

Bakulin, A., R. Burnstad, M. Jervis, and P. Kelamis, 2012, Evaluating permanent seismic monitoring with shallow buried sensors in a desert environment: 82nd Annual International Meeting, SEG, Expanded Abstracts, https://doi.org/10.1190/segam2012-0951.1.

Bakulin, A., R. Smith, M. Jervis, and R. Burnstad, 2015, Use of early arrivals for 4D analysis and processing of buried receiver data on land: 85th Annual International Meeting, SEG, Expanded Abstracts, 5493–5497, https://doi.org/10.1190/segam2015-5749603.1.

Bakulin, A., R. Smith, E. Hemyari, A. Ramadan, M. Jervis, and C. Saragiotis, 2016, Processing and repeatability of 4D buried receiver data in a desert environment: 86th Annual International Meeting, SEG, Expanded Abstracts, 5405–5409, https://doi.org/10.1190/segam2016-13849971.1.

Bakulin, A., P. Golikov, M. Dmitriev, D. Neklyudov, P. Leger, and V. Dolgov, 2018a, Application of supergrouping to enhance 3D prestack seismic data from a desert environment: The Leading Edge, **37**, no. 3, 200–207, https://doi.org/10.1190/tle37030200.1.

Bakulin, A., R. Smith, and M. Jervis, 2018b, Permanent buried receiver monitoring of a carbonate reservoir in a desert environment: 80th Conference and Exhibition, EAGE, Extended Abstracts, https://doi.org/10.3997/2214-4609.201801471.

Bakulin, A., D. Alexandrov, C. Saragiotis, A. Al Ramadan, and B. Kashtan, 2018c, Correcting source and receiver scaling for virtual source imaging and monitoring: Geophysics, **83**, no. 3, Q15–Q24, https://doi.org/10.1190/geo2017-0163.1.

Bergmann, P., A. Kashubin, M. Ivandic, S. Lüth, and C. Juhlin, 2014, Time-lapse difference static correction using prestack crosscorrelations: 4D seismic image enhancement case from Ketzin: Geophysics, **79**, no. 6, B243–B252, https://doi.org/10.1190/geo2013-0422.1.

Berron, C., E. Forgues, A. Bakulin, R. Burnstad, and M. Jervis, 2012, Effects of complex near surface on 4D acquisition with buried source and receiver: 82nd Annual International Meeting, SEG, Expanded Abstracts, https://doi.org/10.1190/segam2012-0937.1.

Bertrand, A., P. G. Folstad, B. Lyngnes, S. Buizard, H. Hoeber, N. Pham, S. de Pierrepont, J. Schultzen, and A. Grandi, 2014, Ekofisk life-of-field seismic: Operations and 4D processing: The Leading Edge, **33**, no. 2, 142–148, https://doi.org/10.1190/tle33020142.1.

Ivanova, A., A. Kashubin, N. Juhojuntti, J. Kummerow, J. Henninges, C. Juhlin, S. Lüth, and M. Ivandic, 2012, Monitoring and volumetric estimation of injected CO_2 using 4D seismic, petrophysical data, core measurements and well logging: A case study at Ketzin, Germany: Geophysical Prospecting, **60**, no. 5, 957–973, https://doi.org/10.1111/j.1365-2478.2012.01045.x.

Johnston, D. H., 2013, Practical applications of time-lapse seismic data: SEG Distinguished Instructor Short Course, https://doi.org/10.1190/1.9781560803126.

Kragh, E., and P. Christie, 2002, Seismic repeatability, normalized rms, and predictability: The Leading Edge, **21**, no. 7, 640–647, https://doi.org/10.1190/1.1497316.

Li, X., R. Couzens, J. R. Grossman, and K. Lazorko, 2012, Simultaneous time-lapse processing for improved repeatability: First Break, **30**, no. 10, 107–110.

Lumley, D., D. C. Adams, M. Meadows, S. Cole, and R. Wright, 2003, 4D seismic data processing issues and examples: 73rd Annual International Meeting, SEG, Expanded Abstracts, 1394–1397, https://doi.org/10.1190/1.1817550.

Meadows, M. A., and S. P. Cole, 2013, 4D seismic modeling and CO_2 pressure-saturation inversion at the Weyburn Field, Saskatchewan: International Journal of Greenhouse Gas Control, **16**, S103–S117, https://doi.org/10.1016/j.ijggc.2013.01.030.

Pevzner, R., V. Shulakova, A. Kepic, and M. Urosevic, 2011, Repeatability analysis of land time-lapse seismic data: CO2CRC Otway pilot project case study: Geophysical Prospecting, **59**, no. 1, 66–77, https://doi.org/10.1111/j.1365-2478.2010.00907.x.

Pevzner, R., M. Urosevic, D. Popik, K. Tertyshnikov, E. Caspari, J. Correa, A. Kepic, et al. 2017, Seismic monitoring of CO2 geo-sequestration: Preliminary results from Stage 2C of the CO2CRC Otway Project one year post injection: 87th Annual International Meeting, SEG, Expanded Abstracts, 5895–5900, https://doi.org/10.1190/segam2017-17670937.1.

Qin, F., P. C. Leger, J. Ren, V. Aleksic, R. W. Rowe, S. Zainaldin, and S. A. Hadab, 2018, A robust implementation and application of antileakage Fourier transform interpolation: The Leading Edge, **37**, no. 7, 538–543, https://doi.org/10.1190/tle37070538.1.

Roach, L. A. N., D. J. White, and B. Roberts, 2015, Assessment of 4D seismic repeatability and CO_2 detection limits using a sparse permanent land array at the Aquistore CO_2 storage site: Geophysics, **80**, no. 2, WA1–WA13, https://doi.org/10.1190/geo2014-0201.1.